

PACS numbers: 42.55.Wd; 42.60.Da; 42.60.Mi
DOI: 10.1070/QE2009v039n10ABEH014139

Low frequency noise distributed-feedback ytterbium fibre laser

M.A. Nikulin, S.A. Babin, A.K. Dmitriev, A.S. Dychkov,
S.I. Kablukov, A.A. Lugovoy, Yu.Ya. Pecherskii

***Abstract*. We report a single-frequency 1-W fibre laser source emitting at 1093 nm, composed of a distributed-feedback ytterbium fibre laser and fibre-optic amplifier. The laser frequency was stabilised by side-locking to a transmission peak of a Fabry–Perot interferometer, and the residual frequency noise spectrum of the laser was measured. Our results indicate that the laser linewidth can be narrowed down below 1 kHz.**

Keywords: *single-frequency lasers, DFB lasers, fibre lasers, fibre-optic amplifiers, frequency noise.*

1. Introduction

Distributed-feedback (DFB) fibre lasers [1] are attractive single-frequency light sources for a number of applications where a narrow linewidth of the laser output spectrum or, in other words, a large coherence length is critical. Examples include coherent optical sensors, ultrahigh-resolution spectrometers and light sources for precision physical experiments. In particular, frequency-doubled ytterbium-doped DFB fibre lasers were used in iodine spectroscopy near 515 [2] and 546 nm [3], and their fourth harmonic was used in laser cooling of Mg^+ [4].

The cavity of a DFB laser is a refractive index or gain Bragg grating induced in the active medium. Such cavities were first used in dye lasers [5, 6]. Early work, including that on DFB semiconductor lasers, was reviewed in paper [7]. A quarter-wave phase shift in the middle of the cavity ensures selection of a single longitudinal mode [8], which makes DFB lasers exceptionally stable single-frequency light sources. A DFB fibre laser is a fibre Bragg grating (FBG) several centimetres in length inscribed in a single-mode optical fibre doped with rare-earth ions (Er, Er/Yb, Yb or Tm). DFB fibre lasers have a smaller gain, a longer cavity, and narrower intrinsic emission linewidth in comparison with DFB semiconductor lasers.

Consider in greater detail the optical emission spectrum of DFB fibre lasers. Rønnekleiv [9] used a general laser theory to describe their response to various perturbations, including relaxation oscillations. He examined the effect of pump modulation on the output power and frequency of an erbium-doped fibre DFB laser and interpreted the results in terms of a thermal variations in the refractive index. The decrease in the relative intensity noise by te feedback from the DFB laser power detector to the pump laser diode current resulted in suppression of the relaxation oscillation peak in the intensity and frequency noise spectra. At high frequencies, the measured frequency noise spectrum was consistent with the thermal noise model for heat transport fluctuations. The $1/f$ dependence in the low frequency region of the frequency noise spectra was later associated with the random character of the heat release accompanying spontaneous emission of the erbium ion [10].

Simonsen et al. [11] demonstrated frequency locking of an Er-doped fibre laser to an absorption line of CO_2. The frequency was adjusted using a piezoelectric transducer stretching the cavity and, accordingly, varying the FBG period. A similar approach was proposed by Cranch [12]: one of two independent optical-fibre Mach–Zehnder interferometers was used to stabilise the output phase of an erbium-doped fibre DFB laser, and the other, to measure the phase noise. Cliche et al. [13] reported a linewidth reduction to 6 Hz, achieved by locking an erbium-doped fibre DFB laser to a fibre Michelson interferometer.

In this paper, we report a single-frequency master oscillator–power amplifier based on a 1093-nm ytterbium fibre DFB laser and a fibre-optic amplifier with an output power of 1 W. The frequency of the master oscillator was stabilised through feedback to the pump power, and we studied the spectral properties of the resultant source. The laser was designed to pump a parametric oscillator with the aim of creating an optical frequency standard.

2. Single-frequency fibre laser source

A schematic of the single-frequency fibre laser source is shown in Fig. 1. Its spectral properties are determined primarily by the DFB fibre laser. The laser cavity was produced by inscribing an about 4-cm-long Bragg grating, with a quarter-wave phase shift in its middle, into an ytterbium-doped optical fibre using the UV radiation from

M.A. Nikulin, S.A. Babin, S.I. Kablukov Institute of Automation and Electrometry, Siberian Branch, Russian Academy of Sciences, prosp. Akad. Koptyuga 1, 630090 Novosibirsk, Russia; Novosibirsk State University, ul. Pirogova 2, 630090 Novosibirsk, Russia;
e-mail: nikulin@iae.nsk.su;
A.K. Dmitriev, A.S. Dychkov, A.A. Lugovoy Institute of Laser Physics, Siberian Branch, Russian Academy of Sciences, prosp. Akad. Lavrent'eva 13/3, 630090 Novosibirsk, Russia;
e-mail: lugovoy@laser.nsc.ru;
Yu.Ya. Pecherskii Institute of Semiconductor Physics, Siberian Branch, Russian Academy of Sciences, prosp. Akad. Lavrent'eva 13, 630090 Novosibirsk, Russia; e-mail: pecher@isp.nsc.ru

Received 10 April 2009
Kvantovaya Elektronika **39** (10) 906–910 (2009)
Translated by O.M. Tsarev

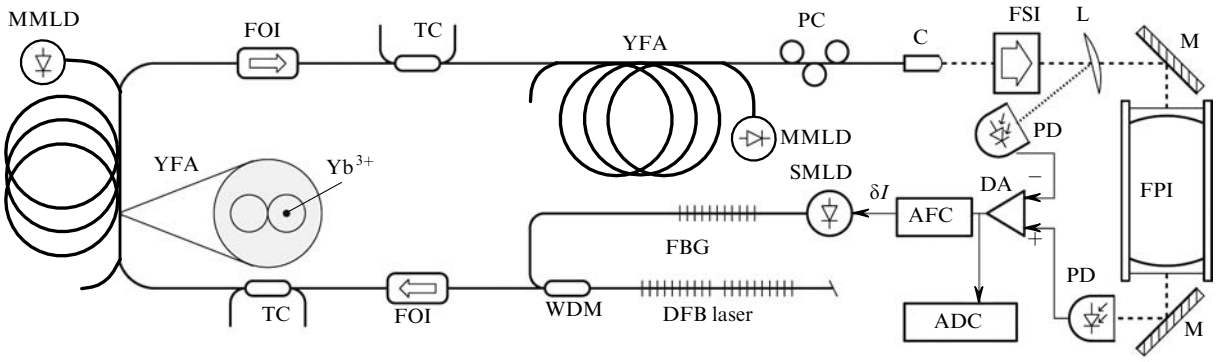

Figure 1. Schematic diagram of the single-frequency fibre laser source: (WDM) wavelength-division multiplexer; (SMLD) and (MMLD) single-mode and multimode laser diodes; (FOI) polarisation insensitive fibre-optic isolator; (TC) low-ratio tap coupler; (YFA) ytterbium fibre amplifier; (PC) polarisation controller; (C) collimator; (FSI) free space isolator; (L) matching lens; (M) mirror; (FPI) Fabry Perot interferometer; (PD) photodiode; (DA) differential amplifier; (ADC) analogue-to-digital converter; (AFC) automatic frequency control.

a frequency-doubled argon ion laser. The DFB laser was pumped by an FBG-stabilised single-mode laser diode (SMLD) with an output power of up to 150 mW, operating at 976 nm, that is, at the absorption maximum of the Yb^{3+} ion [14]. The laser was described in greater detail elsewhere [15, 16].

In the first experiments, the active fibre was exposed to air and was fixed at the ends of the distributed laser cavity. As in the case of Er : Yb fibre lasers [17], pump power absorption in the active fibre was accompanied by a rise in its temperature, nonuniform along the length of the cavity, and thermal distortion of the FBG. With increasing pump power, this led to output power saturation at a level of about 0.5 mW. The optimum pump wavelength was about 970 nm [16], which corresponds to the slope of the absorption peak of the ytterbium ion. In addition, heating the fibre influenced the lasing wavelength (as in the case of Er : Yb fibre lasers [18]), with a proportionality coefficient of $\sim 1.4 \times 10^{-3}$ nm mW^{-1}.

Fixing the laser cavity to an aluminium heatsink improved heat removal, thereby eliminating power saturation and raising the output power to 6 mW, which was then limited by the available pump power. At the same time, the effect of pump power on the lasing wavelength became markedly weaker, with a slope of 2.5×10^{-4} nm mW^{-1}, or 40 kHz per microampere of the laser diode pump current. When secured to the heatsink, the fibre was noticeably less sensitive to acoustic noise and vibrations, so only this configuration will be considered below.

To raise the single-frequency power from several milliwatts to 1 W, a two-stage ytterbium fibre amplifier (YFA) was spliced to the output of the DFB master oscillator. Since the Yb^{3+} ion has a small 1093-nm absorption cross section [14], amplification is possible at low pump intensity. Increasing the population inversion of the ytterbium levels leads to an undesirable increase in the amplified spontaneous emission at wavelengths near the maximum in the stimulated emission cross section (about 1025 nm), thereby reducing the signal-to-noise ratio. The optimal, low Yb^{3+} excited-state population can be ensured by cladding-pumping the active fibre with multimode laser diodes (MMLDs).

The two stages of the amplifier are made from multiple-first-cladding fibre [19], which ensures a reliable all-fibre configuration requiring no tuning. A low refractive index polymer cladding encases two silica fibres in optical contact with one another. One fibre is for delivering a pump wave. The core of the other fibre is doped with ytterbium and amplifies the signal. The gain in both YFA stages is limited by parasitic reflection and scattering (stimulated Brillouin and Rayleigh scattering) in the fibre. To suppress the coupling between the amplifier stages and rule out their influence on the master oscillator, the setup includes fibre-optic isolators. The free space isolator at the output of the source (collimator) suppresses the reflection from the Fabry Perot interferometer in the measuring circuit.

The amplifier configuration ensures about 100-mW and 1-W output powers in the first and second stages at pump powers of 1.7 and 3 W, respectively. The relatively low efficiency is not critical at this power level and is determined by the following factors: The initial portion of the first stage operates in an unsaturated regime, and the active fibre is not long enough to absorb all of the pump power. In some sense, this is a compromise intended to ensure a low inverse population of the Yb^{3+} levels at a limited integral gain. The efficiency of the second amplifier stage is determined largely by the fibre splice loss due to imperfect mode field matching of the active fibre and the fibre at the amplifier input and output. Both amplifier stages operate in the saturated regime relative to the input signal, and their output power is a linear function of the pump power. The performance parameters of the amplifiers and their design were described in greater detail elsewhere [20].

Thus, using an ytterbium fibre DFB laser in combination with a fibre-optic amplifier, we obtained single-frequency lasing at 1093 nm with 1-W output power.

3. Laser frequency stabilisation

To incorporate the single-frequency laser under consideration into an optical frequency standard, a high laser frequency stability is needed. We used one of the simplest active stabilisation methods, which requires no high-bandwidth electronics and allows for spectral noise analysis.

The laser beam (Fig. 1) was directed through a matching lens to a confocal Fabry Perot interferometer with a 53-cm base and a resonance linewidth of about 1 MHz. The laser frequency was side-locked to a transmission peak of the interferometer at its steepest slope point. The power of the beam passed through the interferometer was measured by a

photodiode. Another photodiode detected the beam reflected from the lens and was used to monitor the input power. Adjusting the gains of the channels in the differential amplifier (DA), we were able to suppress the power fluctuation contribution to the difference signal between the laser frequency and stabilisation point. The frequency detuning signal was fed to an automatic frequency control (AFC) system.

As shown earlier [15], the output frequency of the laser under consideration depends on the pump power. This effect was used to stabilise the frequency: the AFC system controlled the current through the SMLD that pumped the DFB fibre laser. Figure 2 shows the frequency response of the laser to SMLD current modulation. As seen, the AFC bandwidth may reach several tens of kilohertz, which is comparable to parameters achievable when the laser frequency is controlled by a piezoelectric transducer. One advantage of pump power control is that the fibre is free of mechanical influences.

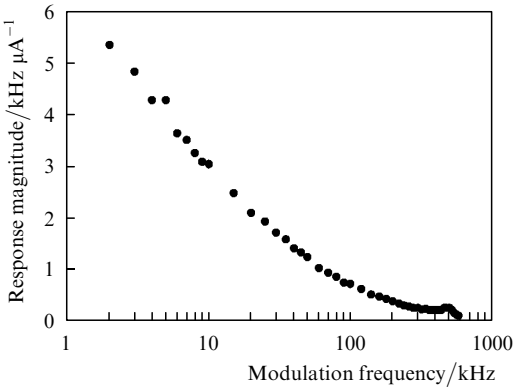

Figure 2. Frequency response of the laser to SMLD pump current modulation.

Pump radiation may influence the refractive index of the active fibre and, hence, the laser output frequency through several mechanisms. The nonlinear effects in silica glass are too weak to be responsible for the observed behaviour. Besides, one would expect an almost flat frequency response in the frequency range studied. Ytterbium ion redistribution between energy levels is of importance for optical amplifiers [21]. The round-trip saturated gain of the laser and, hence, the fraction of excited ions are determined by the total loss in the cavity. DFB lasers may exhibit effects related to the influence of the pump power on the longitudinal mode profile and cavity loss. Moreover, pump power absorption followed by longer wavelength emission may lead to heating of the fibre. This mechanism is supported, e.g., by the above-mentioned weakening of the temperature effect with increasing heat removal and by the agreement with the thermal model for erbium lasers [9].

One common approach for tuning the laser wavelength over the range 0.5 – 1 nm and the slow AFC loop is to control the temperature of the heatsink to which the DFB laser cavity is fixed. The increase in the refractive index of the fibre with increasing temperature and the contribution from the linear expansion of the heatsink with the laser cavity give the dependence represented in Fig. 3.

Thus, we developed a DFB fibre laser frequency control system with a fast loop based on pump SMLD current

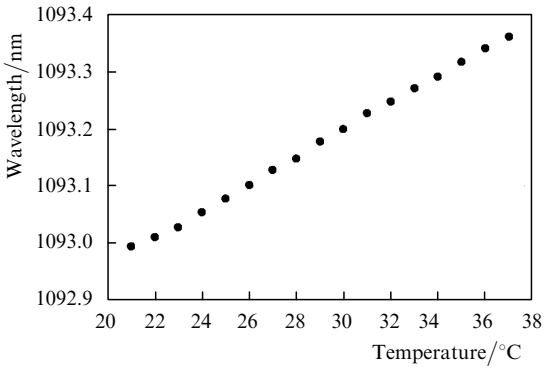

Figure 3. DFB laser wavelength vs. temperature of the heatsink with the laser cavity.

control. Slow frequency tuning can be performed by varying the temperature of the laser cavity.

4. Spectral characteristics

The key parameters of lasers for spectroscopic and metrological applications are the emission linewidth, determined by residual frequency fluctuations, and the frequency noise spectrum, which provides more information about the AFC system and allows one to analyse the mechanisms of emission line broadening.

We studied the relative frequency stability of the laser locked to an external reference cavity. Achieving the ultimate absolute frequency stability was beyond the scope of this study.

When the laser frequency is side-locked to a transmission peak of a Fabry – Perot interferometer, residual frequency noises convert to power fluctuations at the interferometer output, which offers the possibility to determine the above characteristics. The proportionality factor between power changes and the frequency detuning was evaluated from the slope of the transmission spectrum of the interferometer at the lock point. The time variation of the power at the interferometer output, corresponding to the laser frequency detuning, $\Delta\nu$, was recorded using an L-Card E14-440 ADC at a sampling rate of 100 kHz (10-μs intervals), which allowed us to detect frequency noises up to $f_N = 50$ kHz. Custom-written software made it possible to real-time monitor the frequency noise spectrum as the fast Fourier transform of the series $\Delta\nu_k = \Delta\nu(k\tau)$ and to store the $\Delta\nu_k$ values for subsequent analysis.

Figure 4 compares the spectral noise of the master oscillator [curve (*1*)] and that at the output of the fibre amplifier [curve (*2*)] with an AFC bandwidth narrower than 1 kHz. Distinctions occur mainly at low frequencies, where the amplified signal has harmonics that are multiples of 100 Hz. These peaks are related to the insufficient suppression of mains harmonics in the power supplies of the MMLDs and result from changes in the refractive index of the active fibre due to the pump power variations [21]. After thorough filtration of the mains harmonics in the MMLD current, the optical amplifier will not distort the emission spectrum of the laser at the given sensitivity level of the measuring circuit. Spectrum (*3*) is the result of extending the AFC band to ~ 10 kHz, which ensured low-frequency noise suppression. The increase in the spectral noise in the range 10 – 20 kHz can be understood in

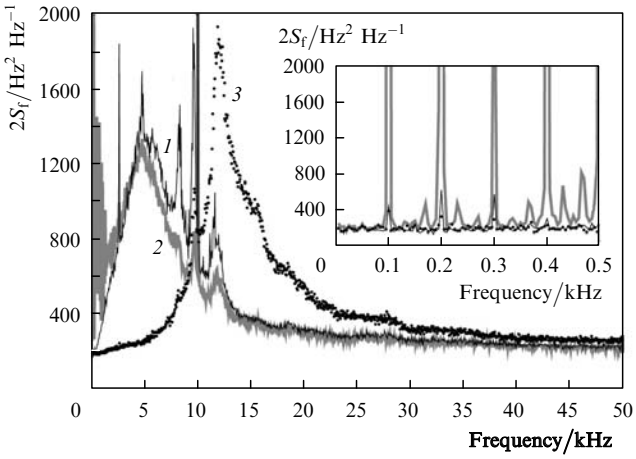

Figure 4. Power spectral density of frequency noise, $2S_f$: (*1*) DFB fibre laser, narrow AFC band; (*2*) amplifier, narrow AFC band; (*3*) amplifier, increased AFC band.

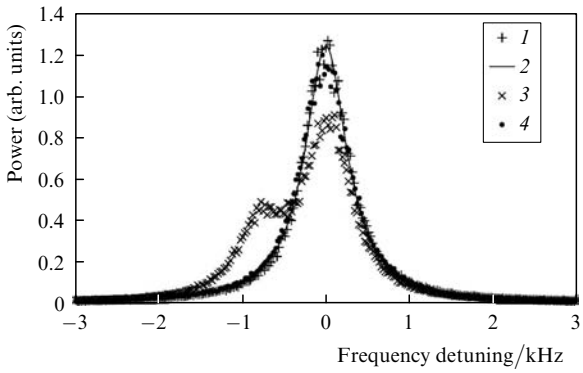

Figure 5. Reconstructed output spectrum of the DFB laser: (*1*) line profile of the master oscillator; (*2*) Lorentzian fit; (*3*) spectrum of the source with the amplifier switched on; (*4*) spectrum with the amplifier switched on, after digital filtration of the 100, 200 and 300 Hz mains harmonics.

terms of the phase characteristics of the AFC used. Note that the characteristics of the laser (Fig. 2) suggest that the AFC band can be extended further.

The constant background in the three spectra is due to the fact that, when digitised, the noise at frequencies above f_N and within the boundary of the band of the photodiodes, amplifiers and AFC input circuits (above 1 MHz) is transferred to the frequency range $0 - f_N$.

The emission spectrum of a laser can be transferred from the optical range to radio frequencies, e.g. by obtaining heterodyne beating with a more stable laser close in frequency. In this way, one can determine the spectral bandwidth of the laser. Similarly, using the time dependence of laser frequency detunings, $\Delta\nu_k$, one can reconstruct the electromagnetic wave field at a frequency ν_0 in the range from 0 to f_N:

$$E_j = E(j\tau) = E_0 \cos\left[2\pi\tau\left(\nu_0 + \sum_{k=0}^{j}\Delta\nu_k\right)\right].$$

The spectrum of the field, obtained via Fourier transformation, corresponds to the laser output spectrum shifted to radio frequencies. Squaring it (to obtain the power spectrum) and averaging the result within the spectral ranges, we obtain the spectra displayed in Fig. 5. The output spectrum of the DFB laser with the amplifier switched off [spectrum (*1*)] is well represented by a Lorentzian [curve (*2*)] with a full width at half maximum of 0.61 kHz. Switching on the amplifier pump diodes [spectrum (*3*)] leads to spectral distortions due to the mains harmonics in the MMLD current. Suppressing the 100, 200, and 300 Hz harmonics by digital filtration before reconstructing the electric field phase reproduces the original laser output spectrum [spectrum (*4*)].

The observed spectral shape and width are determined not only by the laser frequency noise but also by the noise transfer from the frequency range above f_N, nonoptimality of the phase characteristic of the AFC system and slow drift of the AFC and ADC levels. The contribution of laser amplitude noise to the measured frequency noise is small, about 7.7 $Hz^2\ Hz^{-1}$.

It is also worth noting that laser frequency locking and spectral noise measurements using the same Fabry–Perot interferometer allow one to assess only the stabilisation accuracy and frequency noise suppression. The actual linewidth and long-term stability are determined by the parameters of the reference cavity. To achieve the ultimate performance, frequency locking of the single-frequency laser to a quantum reference is planned.

Thus, residual frequency noise spectra were measured using a Fabry–Perot interferometer, and the output spectrum of the laser was shown to be less than 1 kHz in width. Within the sensitivity level reached, the fibre amplifier makes no contribution to the noise provided there is sufficient stabilisation of the current through the amplifier pump diodes.

5. Conclusions

The described distributed-feedback ytterbium fibre laser provides a single-frequency output at 1093 nm, and the two-stage fibre-optic amplifier raises the output power to 1 W. To demonstrate frequency stabilisation, the frequency of the laser source was side-locked to a transmission peak of the Fabry–Perot interferometer and was adjusted by controlling the pump power. To assess the spectral characteristics of the source, we measured frequency noise spectra. The results demonstrate that active stabilisation ensures a residual laser linewidth below 1 kHz.

The output wavelength and power of the laser source are suitable for pumping a parametric oscillator to give narrowband radiation near 3.28 μm, corresponding to the R(2) ν_3 methane line. Our results suggest that the single-frequency source is suitable for spectroscopic applications and for designing a next-generation optical frequency standard based on methane transitions.

Acknowledgements. This work was supported by the RF Ministry of Education and Science, the RF President's Grants Council for Support to Leading Scientific Schools (Grant No. NSh-1527.2008.2) and the Russian Foundation for Basic Research (Grant No. 06-02-16989). We also acknowledge the support from the Siberian Branch of the Russian Academy of Sciences through an integrated research programme, Physical Sciences Division, and Presidium of the Russian Academy of Sciences.

References

1. Kringlebotn J.T., Archambault J.-L., Reekie L., Payne D.N. *Opt. Lett*., **19**, 2101 (1994).
2. Wallerand J.-P., Robertsson L., Ma L.-S., Zucco M. *Metrologia*, **43**, 294 (2006).
3. Markert F., Scheid M., Kolbe D., Walz J. *Opt. Express*, **15**, 14476 (2007).
4. Friedenauer A., Markert F., Schmitz H., Petersen L., Kahra S., Herrmann M., Udem TH., Hänsch T.W., Schätz T. *Appl. Phys. B*, **84**, 371 (2006).
5. Kogelnik H., Shank C.V. *Appl. Phys. Lett*., **18**, 152 (1971).
6. Shank C.V., Bjorkholm J.E., Kogelnik H. *Appl. Phys. Lett*., **18**, 395 (1971).
7. Luk'yanov V.N., Semenov A.T., Shelkov N.V., Yakubovich S.D. *Kvantovaya Elektron*., **2**, 2373 (1975) [*Sov. J. Quantum Electron*., **5**, 1293 (1975)].
8. Haus H.A., Shank C.V. *IEEE J. Quantum Electron*., **12**, 532 (1976).
9. Rønnekleiv E. *Opt. Fiber Technol*., **7**, 206 (2001).
10. Foster S. *Phys. Rev. A*, **78**, 013820 (2008).
11. Simonsen H., Henningsen J., Søgaard S. *IEEE Trans. Instr. Meas*., **50**, 482 (2001).
12. Cranch G.A. *Opt. Lett*., **27**, 1114 (2002).
13. Cliche J.-F., Allard M., Têtu M. *OAA/COTA* (Whistler, Canada, 2006) CFC5.
14. Mel'kumov M.A., Bufetov I.A., Kravtsov K.S., Shubin A.V., Dianov E.M. *Kvantovaya Elektron*., **34**, 843 (2004) [*Quantum Electron*., **34**, 843 (2004)].
15. Babin S.A., Churkin D.V., Kablukov S.I., Nikulin M.A. *Proc. SPIE Int. Soc. Opt. Eng*., **6727**, 672716 (2007).
16. Babin S.A., Churkin D.V., Ismagulov A.E., Kablukov S.I., Nikulin M.A. *Laser Phys. Lett*., **4**, 428 (2007).
17. Dong L., Loh W.H., Caplen J.E., Minelly J.D., Hsu K., Reekie L. *Opt. Lett*., **22**, 694 (1997).
18. Horak P., Voo N.Y., Ibsen M., Loh W.H. *IEEE Photonic. Technol. Lett*., **18**, 998 (2006).
19. Bufetov I.A., Bubnov M.M., Mel'kumov M.A., Dudin V.V., Shubin A.V., Semenov S.L., Kravtsov K.S., Guryanov A.N., Yashkov M.V., Dianov E.M. *Kvantovaya Elektron*., **35**, 328 (2005) [*Quantum Electron*., **35**, 328 (2005)].
20. Babin S.A., Chirkin D.V., Kablukov A.S., Nikulin M.A. *Laser Phys*., **17**, 1292 (2007).
21. Fotiadi A.A., Antipov O.L., Mégret P. *Opt. Express*, **16**, 12658 (2008).